ISSN (Print) 1226-1750
ISSN (Online) 2233-6656
**Journal of Magnetics** 26(1), 25-31 (2021) https://doi.org/10.4283/JMAG.2021.26.1.025

# Load-Carrying Capacity Prediction of Magnetic Fluid Hydrodynamic Bearing Under External Magnetic Field

**Yaqi Zhao, Jianmei Wang*, Dingbang Hou, and Jinsheng Hou**

*Engineering Research Centre of Heavy Machinery Ministry of Education, Taiyuan University of Science and Technology, Taiyuan 030024, China*

(Received 26 August 2020, Received in final form 17 March 2021, Accepted 24 March 2021)

**To decrease the negative influence of the poor working environment on lubricating performance, a new hydrodynamic bearing with magnetic fluid is developed, whose lubricating performance can be significantly improved by external magnetic field. The mathematical model of magnetic intensity generating by a solenoid, which is designed as external magnetic field, is deduced according to Biot-Savart Law and validated by measurement experiment. The direct relationship of load-carrying capacity of bearing and magnetic intensity of external magnetic field is built, through analyzing the effect of magnetic flux density on magnetic fluid viscosity. The results showed that solenoid is reasonable to apply as external magnetic field, and its theory works. Magnetic intensity of external magnetic field can enhance and monitor the bearing load-carrying capacity until magnetic fluid reaches magnetic saturation.**

**Keywords :** hydrodynamic bearing, magnetic fluid, magnetic intensity, external magnetic field, load-carrying capacity, lubrication

## 1. Introduction

As the main part of rolling mill, hydrodynamic bearing plays a vitally important role in rolling machinery and its running stability directly affects working performance of rolling machinery [1]. Failure of the bearing is always related to characters of lubricant which exist between shaft and bearing bush. When temperature rise, oil viscosity decrease, oil film become thinner or even rupture [2-4]. Therefore, ferrofluid has now been used as lubricant to improve lubricating performance of hydrodynamic bearing [5-7].

As a new type of lubricant, ferrofluid not only possesses liquidity but also has magnetism. With external magnetic field, characteristics of ferrofluid are improved, such as improvement of viscosity and load-carrying capacity. But the application of ferrofluid to lubrication is not mature, so the researches on ferrofluid used in lubrication is pretty necessary [8-11].

Till now, many experts and scholars have done masses of researches about ferrofluid lubrication under external magnetic flied. Magnetic intensity producing by external magnetic field can improve lubrication performance of the bearing [12-14]. Tze-Chi Hsu showed that magnetic field seriously affected lubrication characteristic of short journal bearing [15]. Hu *et al.* indicated that magnetic field distribution had influence on the bearing load-carrying capacity [16].

In this paper, the mathematical model of magnetic intensity of a solenoid is calculated, which is more concise and visual than the formulas in literature [23]. And the influence of magnetic intensity on viscosity of ferrofluid is analyzed. Then the direct relationship of magnetic intensity and load-carrying capacity of bearing was obtained. The study shows that the mathematical model of magnetic intensity generating by solenoid in this work has better accuracy, and magnetic field generating by solenoid can improve the lubrication environment. The magnetic intensity generating by external magnetic field, can enhance and monitor the load-carrying capacity of magnetic fluid hydrodynamic bearing in a certain condition.

## 2. Theory and Methods

### 2.1. Calculation on magnetic field


*Corresponding author: Tel: +86-186-3514-9106
Fax: +86-0351-2503969, e-mail: wjmhdb@163.com

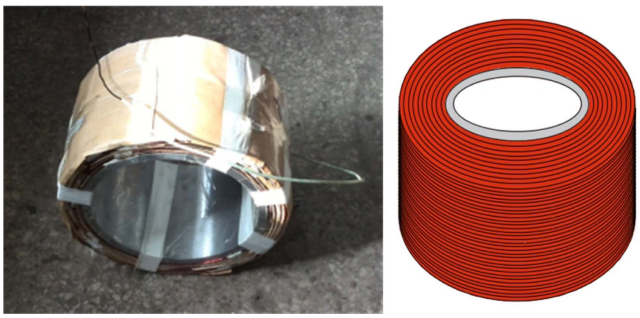

**Fig. 1.** (Color online) The designed solenoid.

Based on the large-scale oil-film bearing test rig, a steel drum was selected, of which size is close to the actual size of the test bearing. Using the drum as the bush, a solenoid was manufactured on CA6140 lathe. The manufactured solenoid is shown in Fig. 1, and the relative parameters are shown in Table 1.

Applying the solenoid in Fig. 1, firstly, the magnetic induction intensity, which is produced by an arbitrary current element on a single-coil, is calculated according to Biot-Savart law. And then the magnetic induction intensity generating by a single coil is deduced through integral algorithm. Finally, induction magnetic intensity of solenoid is obtained based on integral and approximation algorithm. All processes were done in Cartesian coordinate system.

As shown in Fig. 2, a single-coil model is displayed with the center point $O$ as its origin. According to Boit-Savart law, magnetic flux density creating by an arbitrary current element to any outside point N is obtained as follows:

$$d\boldsymbol{B}=\frac{\mu_0 IR}{4\pi}\frac{(R-y\sin\theta)\vec{i}+x\sin\theta\vec{j}+x\cos\theta\vec{k}}{\left(x^2+y^2+R^2-2Ry\sin\theta\right)^{3/2}}d\theta \tag{1}$$

where $I$ is the current in the single coil, $R$ is the radius of the single coil, $\mu_0$ is the vacuum permeability, $\theta$ is the angle between lines OM and z-axis.

With Cartesian coordinate system, $d\boldsymbol{B}$ was decomposed in three directions of $x$, $y$, $z$ to simplify the following calculation. The magnetic induction intensity along the circumference is zero ( $d\boldsymbol{B}_z=0$ ) due to symmetrical structure of the bearing.

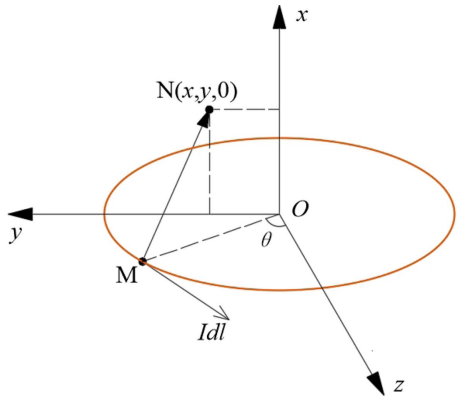


**Fig. 2.** (Color online) Single coil calculation model.

$$d\boldsymbol{B}_x=\frac{\mu_0 IR}{4\pi}\times\frac{R-y\sin\theta}{\left(x^2+y^2+R^2-2Ry\sin\theta\right)^{3/2}}d\theta \tag{2}$$

$$d\boldsymbol{B}_y=\frac{\mu_0 IR}{4\pi}\times\frac{x\sin\theta}{\left(x^2+y^2+R^2-2Ry\sin\theta\right)^{3/2}}d\theta \tag{3}$$

And integral operation and approximation method were applied on Eq. (2) to deduce magnetic induction intensity of the single coil along the axial direction. In the same way, magnetic induction intensity of the single coil intensity of the single coil along the radial direction was got by using integral operation and Taylor Formula on Eq. (3).

$$B_{0x}=\frac{5\mu_0 IR^2}{12\left(x^2+y^2+R^2\right)^{3/2}} \tag{4}$$

$$B_{0y}=\frac{3\mu_0 IR^2 xy}{4\left(x^2+y^2+R^2\right)^{5/2}} \tag{5}$$

The solenoid calculation model is presented in Fig. 3. The sum of magnetic induction intensity producing by every single coil is the magnetic induction intensity of solenoid. This process was calculated by using integral operation and approximation method on Eq. (4) and Eq. (5).

$$B_{1x}=3\mu_0 In_1n_2\left[\begin{array}{l}(L-x)(A-B)+(x+L)(C-D)\\+\frac{y^2}{2}\bullet\ln\frac{(L-x+A)(L-x-B)(L+x+C)(L+x-D)}{(L-x-A)(L-x+B)(L+x-C)(L+x+D)}\end{array}\right] \tag{6}$$

**Table 1.** The relative parameters of the solenoid.

| Parameter | Value | Parameter | Value |
|---|---|---|---|
| Coil material | Red copper | Length of solenoid $L$ (mm) | 180 |
| Inner radius of solenoid $R_1$ (mm) | 123 | Resistance of solenoid winding (Ω) | 6.2 |
| Outer radius of solenoid $R_2$ (mm) | 154 | Electrical resistivity (Ω/m) | 1.75e-8 |
| Numbers of coil in axial direction | 85 | Coil diameter (mm) | 2 |
| Numbers of coil in radial direction | 14 | Relative permeability | 0.999979 |

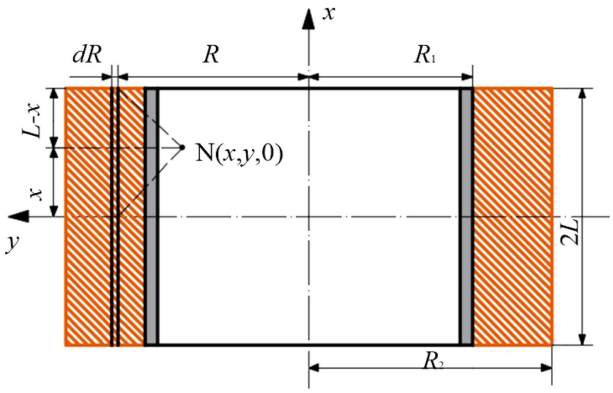


**Fig. 3.** (Color online) Solenoid calculation model.

$$B_{1y}=\frac{\mu_0 I y n_1 n_2}{4}\left[\ln\frac{(R_2+A)(R_1+D)}{(R_1+B)(R_2+C)}+\frac{ACR_1(D-B)+BDR_2(A-C)}{ABCD}\right] \tag{7}$$

where $n_1$ are the number of turns in axial, $n_2$ are the number of turns in radial, $R_1$ is the inner radius of multilayer-turn, $R_2$ is the external radius of multilayer-turn, $A=\sqrt{(x-L)^2+y^2+R_2^2}$, $B=\sqrt{(x-L)^2+y^2+R_1^2}$, $C=\sqrt{(x+L)^2+y^2+R_2^2}$, $D=\sqrt{(x+L)^2+y^2+R_1^2}$

Actually, bush can be magnetized when solenoid works, so magnetic flux density in hydrodynamic bearing is derived by twined wires and magnetized bush. It is assumed that magnetized bush is equivalent to a solenoid, and magnetic intensity producing by bush is opposite to the external solenoid [23]. Therefore, the equations of magnetic induction intensity, along axial and radial directions, in hydrodynamic bearing are modified as follows:

$$B_x=3\mu_0\delta I n_1 n_2\left[\begin{array}{l}\dfrac{(L-x)(A-B)+(x+L)(C-D)}{2}\\ +\dfrac{y^2}{2}\cdot\ln\dfrac{(L-x+A)(L-x-B)(L+x+C)(L+x-D)}{(L-x-A)(L-x+B)(L+x-C)(L+x+D)}\end{array}\right] \tag{8}$$

$$B_y=\frac{\mu_0\sigma I y n_1 n_2}{4}\left[\ln\frac{(R_2+A)(R_1+D)}{(R_1+B)(R_2+C)}+\frac{ACR_1(D-B)+BDR_2(A-C)}{ABCD}\right] \tag{9}$$

where $\sigma$ is a correction factor, $\delta$ is a modified function

$$\delta=\frac{p_1+p_2x+p_3x^2+p_4y+p_5y^2}{1+p_6x+p_7x^2+p_8y+p_9y^2+p_{10}y^3},$$

$\sigma=160\sim180$, $p_1=18.3615$, $p_2=-0.0041$,

$p_3=2750.6644$, $p_4=0.00028$, $p_5=-1943.441$,

$p_6=-7\times10^{-5}$, $p_7=-33.8193$,

$p_8=-6.8663\times10^{-6}$, $p_9=-64.3478$, $p_{10}=-0.001$.

### 2.2. Magnetic induction intensity measure

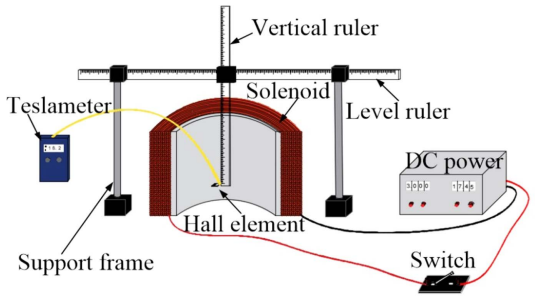


**Fig. 4.** (Color online) Magnetic intensity measurement device.

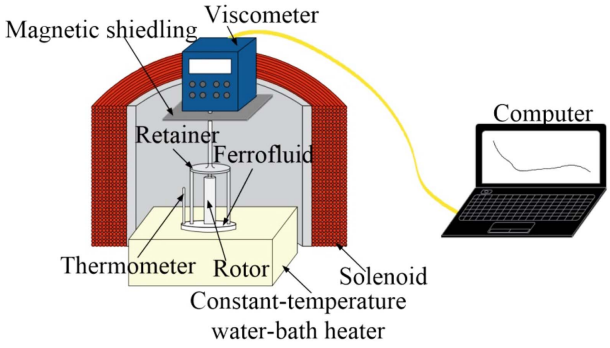


**Fig. 5.** (Color online) Viscosity test device.

The principle of the measurement is based on Hall Effect that the charged particles would be deflected by Lorenz force under magnetic field. A DC power is used to provide current to the solenoid, and a teslameter (WT10A) is applied to test magnetic intensity of a certain point. The point is fixed by two rulers. The measurement device is shown in Fig. 4.

### 2.3. Viscosity test

Figure 5 is the testing equipment to measure the relationship of temperature, magnetic intensity and viscosity. The ferrofluid used in the test is a colloidal suspension including magnetic particles ($Fe_3O_4$) about 6 %, of which size was about 12 nm. A rotational viscometer (NDJ-5S) was used to measure viscosity and the measure results were analyzed on a connected computer. To meet the experimental requirements of various temperature conditions, a constant-temperature water-bath heater was applied, and a thermometer was inserted into the ferrofluid to monitor the real-time temperature. The designed solenoid provides the magnetic intensity through adjusting its current. Viscosity characteristic is tested at 40-70 °C, and the magnetic induction intensity is 10-60 mT.

## 3. Results and Discussion

### 3.1. Analysis of magnetic induction intensity

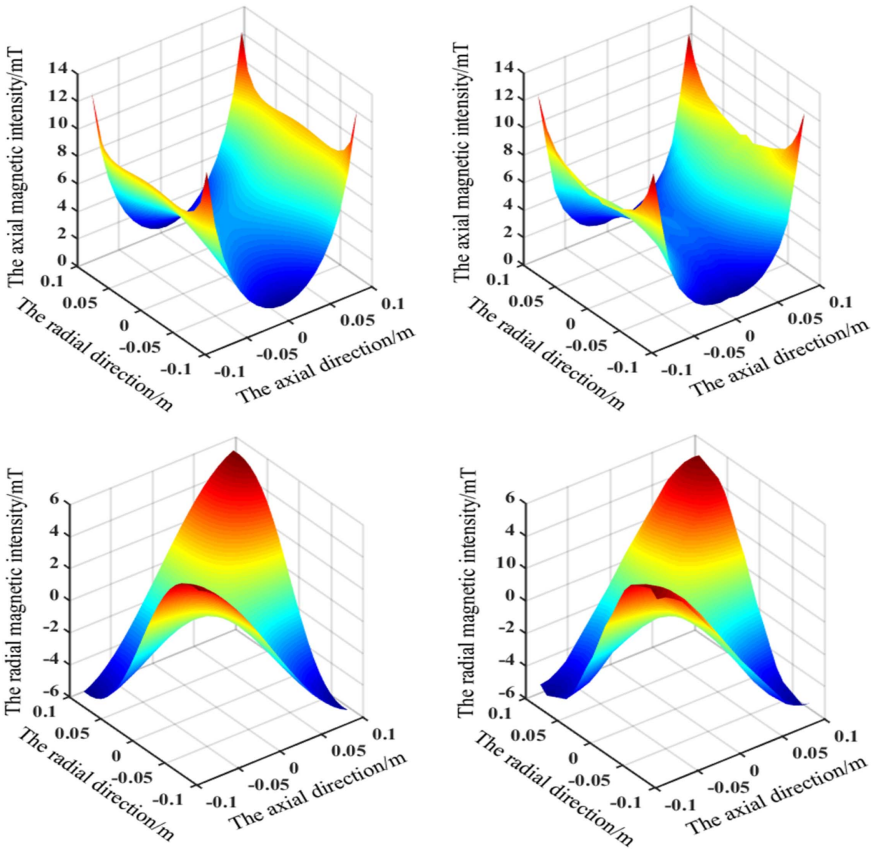


**Fig. 6.** (Color online) Distribution of magnetic induction intensity. (a) Theoretical results of axial magnetic intensity. (b) Experimental results of axial magnetic intensity. (c) Theoretical results of radial magnetic intensity. (d) Experimental results of radial magnetic intensity

Through the above research, the distribution of axial and radial magnetic induction intensity is shown in Fig. 6.

Fig. 6(a) is theoretical result of axial magnetic induction intensity ($B_x$) under 3 A according to the size of the solenoid and the Eq. (8). Fig. 6(b) is experimental result of axial magnetic induction intensity ($B_x$) with the same current. By contrast, the two distributions agree well with each other. $B_x$ reaches the maximum value in the edge of solenoid, and it decreases along the radial direction while increases along the axial direction from the inner center of solenoid. Because the width-diameter ratio of bearing is 0.8, the distribution of magnetic flux density shows no homogeneous where $B_x$ along the axial direction is sharper than the radial direction. The maximum ($B_{x,\max}$) is 12 mT, the minimum ($B_{x,\min}$) is 2 mT.

In the same way, theoretical result of radial magnetic induction intensity ($B_y$) is shown in Fig. 6(c), and Fig. 6 (d) is experimental result. It is obvious that theoretical value is very closer to experimental value. The radial magnetic intensity is zero in the center of solenoid,

**Table 2.** The comparison results of different magnetic intensity mathematical models.

| Results | x | 0.09 | 0.06 | 0.03 | 0 | –0.03 | –0.06 | –0.09 | accuracy |
|---|---|---|---|---|---|---|---|---|---|
| $B_x$ | Modified | 12.7156 | 4.2360 | 1.4984 | 0.7429 | 1.4984 | 4.2360 | 12.7156 | 83.5 % |
| | Literature [23] | 27.0073 | 26.1917 | 25.9441 | 25.7807 | 25.9441 | 26.1917 | 27.0073 | 17.4 % |
| | Experimental | 12.5 | 3.4 | 1.4 | 1.2 | 1.4 | 3.4 | 12.5 | – |
| $B_y$ | Modified | 5.3051 | 4.5942 | 2.5267 | 0 | –2.5267 | –4.5942 | –5.3051 | 93.8 % |
| | Literature [23] | 19.2514 | 15.2532 | 7.635 | 0 | –7.635 | –15.2532 | –19.2514 | 28.3 % |
| | Experimental | 5.1 | 4.5 | 2.2 | 0 | –2.2 | –4.5 | –5.1 | – |

presenting as central-symmetric distribution of which increasing tendency along the axial and radial directions have the similar rate. The maximum is in the edge of solenoid, i.e., $B_{y,\max}$ = 5 mT.

As the agreement of theoretical result and experimental result, the assumption regarding bush as a solenoid is rational.

With comparison with Fig. 6(a) and Fig. 6(c), the axial magnetic induction intensity is bigger than the radial one, it means that the axial magnetic intensity is determinant. The maximal magnetic intensity exists in the edge of the bush, where is the working area of lubricant. It means improving lubrication environment, ensuring the stability of the bearing as well. Thus the equations of magnetic induction intensity deduced in this paper are reasonable and precise. The comparison with two equations in this paper and literature [23] is shown in Table 2.

### 3.2. Viscosity test results

Viscosity is one of the vital parameters to represent the characteristic of lubricating oil. Temperature and pressure are major factors which could affect oil viscosity. Generally, the relationship between viscosity, temperature and pressure is expressed by Einstein formula [17, 18] as follow.

$$\eta_c(P,T)=\eta_{c0}\exp\left\{\frac{(\ln\eta_{c0}+9.67)}{\left[(1+5.1\times10^{-9}\bullet P)^{z}\bullet\left(\frac{T-138}{T_0-138}\right)^{-s}-1\right]}\right\} \quad (10)$$

where $\eta_c$ is viscosity of lubricating oil, $z$ is a viscosity-pressure coefficient, $z$ = 0.68, and $s$ is a viscosity-temperature coefficient, $s$ = 1.1.

According to rotating viscosity theory by Shliomis [19], the equation representing the effect on ferrofluid viscosity by pressure, temperature and magnetic intensity is given as follows:

$$\eta(T,P,B)=\eta_f+\frac{3}{2}\varphi\frac{0.5\alpha L(\alpha)}{1+0.5\alpha L(\alpha)}(\sin^2\beta)\eta_c \quad (11)$$

where $\eta$ is viscosity of ferrofluid with magnetic field, $\eta_f$ is viscosity of ferrofluid without magnetic field, and $\varphi$ is the volume fraction of magnetic particles.

Based on Einstein formula and Rosenweig modification, the relationship between viscosity of ferrofluid and viscosity of carrier fluid can be obtained [20, 21]. Then applying the Langevin function, the viscosity of ferrofluid influenced by magnetic field, temperature and pressure was obtained as follows:

$$\eta(P,T,B)=\eta_{c0}\exp\left\{\frac{(\ln\eta_{c0}+9.67)}{\left[(1+5.1\times10^{-9}P)^{Z}\bullet\left(\frac{T\text{-}138}{T_0\text{-}138}\right)^{-S}-1\right]}\right\}\bullet\left[1+2.5\left(1+\frac{\delta}{r}\right)^{3}\varphi-1.55\left(1+\frac{\delta}{r}\right)^{6}\varphi^2+\frac{1.5k_1}{1/\varphi+3k_0T/\pi r^3\mu_0(\mu_r-1)B^2}\right] \quad (12)$$

where $\delta$ is the thickness of dispersants, $r$ is the radius of magnetic particle, $\mu_0$ is the permeability of vacuum, $M_p$ is magnetization of a single magnetic particle, $k_0$ is Boltzmann constant, $M$ is magnetization of ferrofluid, $k_1$ is a proportion coefficient.

Figure 7 displays the distribution of ferrofluid viscosity changing with temperature and magnetic field intensity. Viscosity of ferrofluid increases with magnetic intensity rise while decreases with temperature rise. And the effect of magnetic field intensity is pretty obvious at lower

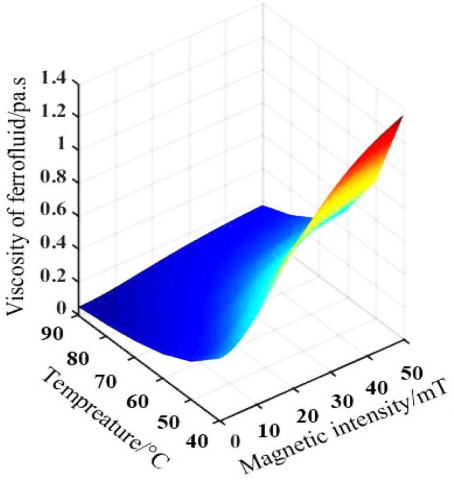


**Fig. 7.** (Color online) Distribution of viscosity under the effects of temperature and magnetic intensity.

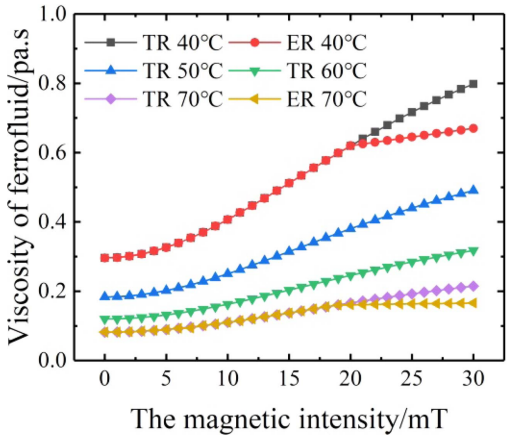


**Fig. 8.** (Color online) The curve of viscosity changing with magnetic intensity. (TR-theoretical result, ER-experimental result)

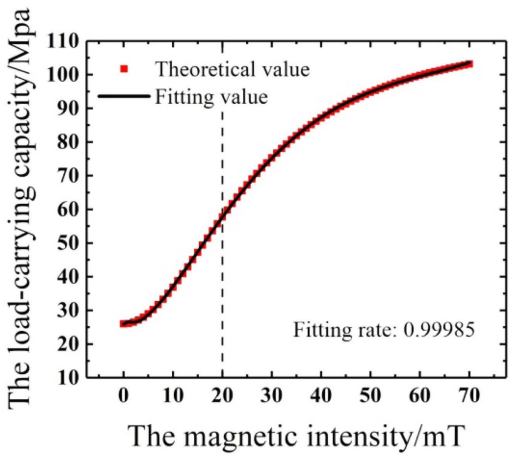


**Fig. 9.** (Color online) Relationship of load-carrying capacity and magnetic intensity.

temperature.

The relationship between ferrofluid viscosity and magnetic intensity is presented in Fig. 8. The rise of magnetic field could effectively improve viscosity, however with the continuously rise of magnetic intensity, viscosity reaches at a stable value in the end. When magnetic intensity arrives at about 20 mT, the curve of viscosity becomes flat. It means that the saturation magnetization of the ferrofluid is 20 mT. Hence magnetic intensity has obvious effect on viscosity of ferrofluid, it could improve viscosity before the ferrofluid approaches saturation point. And we can see, the viscosity decrease with the increasing temperature,

### 3.3. Load-carrying capacity of bearing

Load-carrying capacity is an important parameter to assess the working condition of bearing. Overload would result in the rupture of oil film which easily causes the failure of the bearing, so it is necessary to efficiently increase load-carrying capacity to improve working performance of bearing. According to literature [22], the relationship between load-carrying capacity and viscosity is shown in Eq. (13), which shows that viscosity of lubricant has directly positive influence on load-carrying capacity of bearing.

$$P = k_2 \frac{\omega \eta}{\phi^2} \tag{13}$$

where $\omega$ is the shaft angular velocity, $\phi$ is the relative space of bearing, and $k_2$ is a coefficient related to eccentricity ratio.

When ferrofluid is used instead of traditional lubricant, magnetic induction intensity has positive effect on viscosity, which means magnetic flux density could positively affect load-carrying capacity of ferrofluid hydrodynamic bearing. Combining Eq. (12) with Eq. (13), the relationship between load-carrying capacity and magnetic intensity can be obtained. And a prediction mathematical model of the relationship was calculated by fitting algorithm as well.

$$P = p_1 + p_2 B^{0.5} + p_3 B + p_4 B^{1.5} + p_5 B^2 + p_6 B^{2.5} \tag{14}$$

where $p_1 \sim p_6$ are correlation coefficients.

Figure 9 displays the direct relationship between load-carrying capacity and magnetic intensity. The load-carrying capacity is enhanced as the magnetic intensity increases. A prediction mathematical model was given, and it matched extremely well with theoretical result, which means the prediction mathematical model is rational.

This prediction mathematical model is aim to provide the direct relationship of magnetic intensity and load-carrying capacity in a certain condition. When the bearing is operating, its load-carrying capacity can be adjusted by changing magnetic intensity until lubricant gets magnetic saturation. Further the load-carrying capacity of bearing can be monitored through controlling the value of magnetic intensity, which can improve working performance of the bearing, decline the failure of the bearing.

## 4. Conclusions

(1) A solenoid is designed as external magnetic field for magnetic fluid hydrodynamic bearing. The equation of magnetic induction intensity producing by the solenoid is deduced. And the consistency of theoretical results and experimental results verifies the reasonable of magnetic field model.

(2) The distribution of magnetic induction intensity is uneven but symmetrical, the maximum exists in the working area of lubricant which could improve the lubricating environment of the bearing. The axial magnetic intensity is about three times than the radial ones, which means the axial magnetic intensity is determinant.

(3) The viscosity of ferrofluid is analyzed under magnetic intensity. The magnetic intensity has positive effect on viscosity of magnetic fluid. The theoretical values are in agreement with the experimental results before the ferrofluid approaches to saturation magnetization. When magnetic fluid is fully magnetized, the effect of magnetic field on the viscosity will gradually become slight.

(4) A prediction mathematical model of load-carrying capacity and magnetic intensity is obtained. Through controlling the magnetic intensity can help enhance and monitor the load-carrying capacity of hydrodynamic bearing, thus improving the working performance of the

bearing and decreasing its failure rate.

## Acknowledgements

This work was supported by the National Science Foundation of China [grant numbers 51875382 and U1610109]; Shanxi Provincial Key Research and Development Plan (grant number 201803D421103), Shanxi Provincial Key Science and Technology Special Projects (grant number 20181102023) and the Coordinative Creation Center of Taiyuan Heavy Machinery Equipment.

## References

[1] X. Q. Guo and S. Q. Li, Oil Film Bearing of Modern Large Rolling Mill, China Machine Press, Beijing (1992) pp 5-15.
[2] J. M. Wang, Q. Z. Xia, Y. Ma, F. N. Meng, Y. Liang, and Z. X. Li, Material **10**, 10 (2017).
[3] A. C. Bannwart, K. L. Cavalca, and G. B. Daniel, Mech. Res. Commun **37**, 6 (2010).
[4] T. H. Machado and K. L. Cavalca, Mech. Res. Commun **69**, (2015).
[5] T. A. Osman, G. S. Nada, and Z. S. Safar, Tribol. Lett. **11**, 1 (2001).
[6] P. Kuzhir, Trib. Int. **41**, 4 (2008).
[7] T. A. Osman, G. S. Nada, and Z. S. Safar, Trib. Int **34**, 6 (2001).
[8] J. M. Wang, Z. P. Zuo, Y. Q. Zhao, D. B. Hou, and Z. X. Li, J. Nanosci. Nanotechnol **19**, 5 (2019).
[9] C. Shen, W. Huang, G. L. Ma, and X. L. Wang, Surf. Coat. Tech. **204**, 4 (2009).
[10] K. Parekh, J. Patel, and R. V. Upadhyay, J. Mol. Liq. **248**, (2017).
[11] W. Chen, W. Huang, and X. L. Wang, Trib. Int. **72**, (2014).
[12] J. M. Wang, J. F. Kang, and Y. J. Zhang, Trib. Int. **75**, (2014).
[13] D. Lunz and P. D. Howell, J. Fluid. Mech. 869 (2019).
[14] W. Huang, C. Shen, S. Liao, and X. Wang, Trib. Lett. **41**, 1 (2011).
[15] T. C. Hsu, J. H. Chen, H. L. Chiang, and T. L. Chou, Trib. Int. **61**, (2013).
[16] Z. D. Hu, Z. Wang, W. Huang, and X. L. Wang, Trib. Int. **130**, (2019).
[17] R. T. Lee, K. T. Yang, and Y. C. Chiou, Trib. Int. **66**, (2013).
[18] M. Najjari and R. Guilbault, Trib. Int. **71**, (2014).
[19] R. Patel, R. V. Upadhyay, and R. V. Mehta, J. Colloid. Interface. Sci. **263**, 2 (2003).
[20] Y. Liu, Z. Liu, S. Z. Wen, and Y. B. Xie, Trib. Int. **33**, 12 (2000).
[21] C. Q. Chi, Z. S. Wang, and P. Z. Zhao (Eds), Physics basis and application of ferrofluid, Beihang University Press, Beijing (2011).
[22] Q. X. Huang, G. X. Sheng, and A. S. Liang, Research and Application of Rolling Mill Bearing and Roll Life Metallurgical, Industry Publisher, Beijing (2003).
[23] Y. J. Zhang, J. M. Wang, and D. Li, J. Magn. **22**, 2 (2017).